CAAP Annual Report

Date of Report: *09/30/2024*

Prepared for: *U.S. DOT Pipeline and Hazardous Materials Safety Administration*

Annual Period: **From** *(September 30, 2023)* **to** *(September 29, 2024)*

Contract Number: *693JK32250008CAAP*

Project Title: *Performance Evaluation and Risk Assessment of Excessive Cathodic Protection on Vintage Pipeline Coatings*

Prepared by: *Qixin Zhou and Yuhan Su, Qindan Huang, and Hao Wang*

Contact Info.: *Qixin Zhou, qzhou@uakron.edu, 330-972-7159*
Qindan Huang, qindan.huang@marquette.edu, 414-288-6670
Hao Wang, hw261@soe.rutgers.edu, 848-445-2874

Table of Contents

Section A: Business and Activities

(a) Contract Activities

Contract Modifications: NA

Educational Activities:

- Student mentoring:

  Yuhan Su, a Ph.D. student in Chemical Engineering at The University of Akron is working on the project starting the 2nd quarter of this project.

  Tanner Laughorn, an undergraduate student in Corrosion Engineering at The University of Akron worked on this project from the 5th quarter to the 7th quarter.

  Abbi Acurio, an undergraduate student in Corrosion Engineering at The University of Akron is working on the project starting the 5th quarter of this project.

  Brigida Zhunio Cardenas, a Ph.D. student in Civil, Construction and Environmental Engineering at Marquette University is working on the project starting the 7th quarter.

  Xingsen Yang, a PhD student in Civil Engineering at Rutgers University is working on the project starting the 6th quarter of this project.

- Student internship: NA

- Educational activities:

  The PI (Dr. Zhou) introduced the concept of cathodic protection in the undergraduate course—Introduction to Corrosion Science and Engineering at The University of Akron.

  The PI (Dr. Zhou) introduced corrosion protective coatings in the undergraduate and graduate course—Corrosion Protection by Coatings at The University of Akron.

- Career employed:

  Tanner Laughorn who worked on this project graduated in May 2024 and started his career as a Pipeline Engineer at Burns & McDonnell.

- Others: NA

Dissemination of Project Outcomes: NA

Citations of The Publications: NA

Others:

We received vintage pipes with coating from Dr. Rafael Rodriguez through his company. Dr. Rodriguez kindly provided us with the CP operation potentials and coating information for these pipe samples.

(b) Financial Summary

Federal Cost Activities:

- PI/Co-PIs/students involvement:

  One graduate student from The University of Akron was partially charged from this project for the salary during this reporting period.

  One graduate student from Rutgers University was partially charged from this project for the salary during this reporting period.

  The PI and Co-PIs were charged the summer salary from this project based on the budgeted number.

- Materials purchased/travel/contractual (consultants/subcontractors):

  Materials were purchased for experimental measurement and testing at The University of Akron during this reporting period.

  Travel support was for the graduate student, Yuhan Su, to attend the AMPP 2024 annual conference.

Cost Share Activities:

- Cost share contribution:

  The cost share of Dr. Huang's academic salary from Marquette University has been charged as planned.

(c) Project Schedule Update

Project Schedule:

The proposed research tasks and milestones updated in September 2023 are shown in Table 1. Task 1 is on the schedule and completed. Task 2 is also on the schedule, but we would like to have two more quarters of time to complete the experimental testing. Task 3 is on the schedule. Task 4 just got started. Tasks 4 and 5 need the experimental data from Task 2 and simulation data from Task 3 to generate a database for calculations. It takes more time to wait for the results from Task 2 and Task 3.

Table 1. Schedule and milestones of proposed tasks.

Tasks	Year 1				Year 2				Year 3			
Task 1. Coating & influencing factors identification												
Task 2. Coating performance evaluation												
Task 3. Simulation of coating disbondment & CP												
Task 4. Probabilistic coating degradation model												
Task 5. Recoating time determination												
Task 6. Industrial collaborations												

Corrective Actions:

The updated research tasks and milestones are shown in Table 2. The orange ones are those updated, and the blue ones are those not changed.

Table 2. Updated schedule and milestones of proposed tasks.

Tasks	Year 1				Year 2				Year 3			
Task 1. Coating & influencing factors identification												
Task 2. Coating performance evaluation												
Task 3. Simulation of coating disbondment & CP												
Task 4. Probabilistic coating degradation model												
Task 5. Recoating time determination												
Task 6. Industrial collaborations												

(d) Status Update of the 8th Quarter Technical Activities

Task 1: Identification of vintage pipeline coatings and influencing factors in coating cathodic disbondment (The University of Akron and Marquette University)

Task 1 is in progress this quarter. The Ph.D. student, Yuhan Su, at The University of Akron, is working on literature reviews to understand pipeline coatings and the influencing factors in coating cathodic disbondment. The conditions where the vintage coating experiences cathodic disbondment and the key influencing factors on the cathodic disbondment are studied and taken into the experimental design in Task 2.

Task 2: Evaluation of coating cathodic disbondment considering key influencing factors through laboratory testing (The University of Akron)

The Ph.D. student, Yuhan Su, and the two undergraduate students, Tanner Laughorn and Abbi Acurio, at The University of Akron, are working on this task.

The coating samples under testing this quarter include the liquid epoxy coating as a CP-compatible coating and fusion bonded epoxy (FBE) coating produced by Midwest Coating Company.

The coating cathodic disbondment is studied by applying different cathodic potentials (-

0.775, -1.5, and -2.923 V vs. SCE) under different durations (3, 7, 14, 21 days, 2 months). Each condition is tested for at least three coating samples. The experimental details are described in Section B.

Task 3: Numerical simulation of pipeline coating disbondment behavior and CP system (Rutgers University)

The PhD students at Rutgers University developed an initial model for the simulation of corrosion development with coating disbondment.

Task 4: Probabilistic degradation model of coated pipe wall due to excessive CP (Marquette University)

This Task just got started at Maquette University in the 7th quarter. Dr. Huang is collecting coating disbondment data from different CP conditions for the database to generate the degradation model.

Task 5: Determination of recoating time using reliability-based approach (Marquette University)

Task 5 will start in the 9th quarter of this project.

Section B: Detailed Technical Results in the Report Period

1. Task 1. Identification of Vintage Pipeline Coatings and Influencing Factors in Coating Cathodic Disbondment

1.1. Background and Objectives in the 2nd Annual Report Period

Buried pipelines are protected from corrosion attack by coating and cathodic protection (CP). However, excessive CP could cause serious damage to many types of vintage pipeline coatings, and consequently pipeline integrity.

The objective of Task 1 in this reporting period is to understand the conditions where the vintage coating experiences cathodic disbondment and the key influencing factors on the cathodic disbondment. The experimental design is based on the study of literature review and the survey from pipeline companies.

1.2. Research Progress in the 2nd Annual Report Period

When coating is disbonded at small faults, such as pinholes or holidays, the CP current may be partially or completely shielded, to reach the disbonding crevice, especially at the crevice bottom. As a result, the CP fails to protect the area that is exposed to a corrosive environment. This is called "CP shielding" [1]. Conversely, coatings that do not prevent the distribution of CP current to the steel, are called CP-compatible or CP non-shielding coatings. Generally, widely used coatings like fusion-bonded epoxy (FBE) and coal tar enamel coatings are considered CP-compatible coatings. In contrast, high-performance coating and polyethylene (PE) tape are regarded as CP-shielding coating in the long term.

The coating cathodic disbondment was studied in previous work by applying different CP potentials or CP current densities. The testing procedures or details are specified by the standards of ASTM G8, ASTM G95, NACE TM0115, or other published work, as summarized in Table 3. The conclusion is that the coating cathodic disbondment areas increased as increasing the applied CP potentials [2]. However, previous research papers didn't report the initial and final open circuit potentials (OCP) of these coatings. While we believe this information is very useful for understanding the overprotection of excessive CPs, so we will include OCP monitoring in our experimental design.

Besides CP conditions, previous work studied the CP permeability by applying CP potential [1, 3, 4]. The CP potential applied to the testing coating sample is done through the DC power supply without a reference electrode, which means it cannot guarantee the applied value is the intended value. So, our experimental design will introduce a reference electrode into the experimental setup and associated modifications based on previous studies.

The evolution of coating disbondment area was not often studied in previous work [2, 5]. Although some works considered different time periods of applied CP, they didn't count it as a key factor in coating cathodic disbondment. Our experimental design will couple different CP levels with different duration time to systematically study coating cathodic disbondment.

Table 3. CP conditions used in previous coating cathodic protection studies.

CP Conditions	Reference	Notes
-1.3 V vs SCE	[6]	Pulse current + direct current
-1.4 V vs SCE		
-1.5 V vs SCE		
-1.5 V	[7]	Canada Z245-20-10; not mention the RE
-0.875 V vs SCE	[3]	AC current density (0-500)
-1.5 V vs SCE	[8]	ASTM G8
-0.9~-1.5 V vs SCE	[2]	
-1.5 V vs SCE	[9]	ASTM G95
-1.38 +- 0.02 V vs Ag/AgCl	NACE TM0115	-1.399 V vs SCE
-1.45~1.55 V vs CSE	ASTM G8	-1.373~-1.473 V vs SCE
-3 V vs CSE	ASTM G95	-2.923 V vs SCE

1.3. Company Survey

A survey was sent to industrial companies who were interested in this project through the network of PRCI. The survey aims to obtain field information from pipeline industry partners. These companies took the survey: SoCalGas, Flint Hills Resources, Boardwalk Pipeline, Marathon Pipe Line LLC, and ATCO. The coatings used in the vintage pipelines included almost all types of pipeline coatings, but the coatings used within the recent 20 years mainly are fusion bonded epoxy and FBE. All five companies reported that they experienced coating cathodic disbondment issues. The details of the survey are included in Appendix 1.

1.4. Conclusions

Through the literature reviews, the conditions for pipeline coatings that experience cathodic disbondment are studied and understood. The survey from pipeline companies also provides additional information on coatings and CP conditions in the field. The experimental design in Task 2 will be constructed based on the study of the literature review and the survey. This task is completed.

2. Task 2. Evaluation of Coating Cathodic Disbondment Considering Key Influencing Factors through Laboratory Testing

2.1. Background and Objectives in the 2nd Annual Report Period

A systemic coating performance evaluation will be designed and conducted through experimental testing to study coating cathodic disbondment considering key influencing factors.

The objective of Task 2 in this reporting period is to select coating types, prepare coating samples, and design experiment setups and testing protocols to study coating cathodic disbondment.

2.2. Research Progress in the 2nd Annual Report Period

2.2.1. Experimental design

The experimental design on the evaluation of coating cathodic disbondment includes the selection of coating, the selection of metal, solution, CP level, and characterization method, as summarized in Figure 1. Each item in the experimental design will be discussed below.

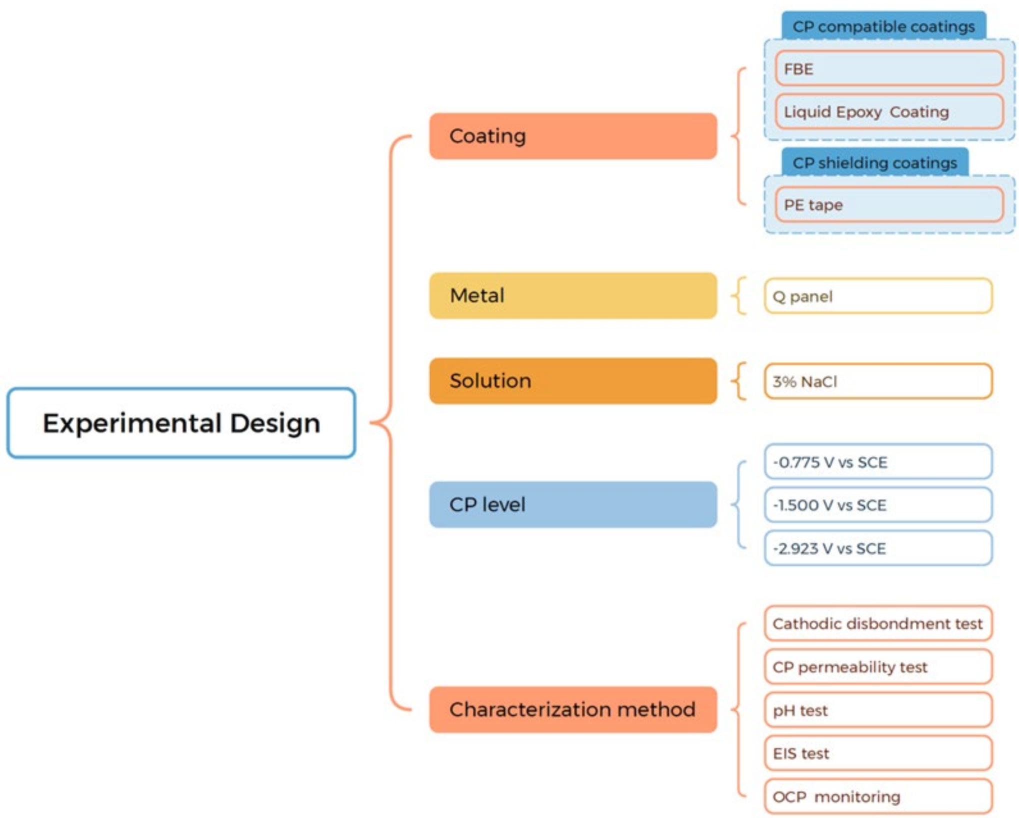

Figure 1. Experimental design for the study of coating cathodic disbondment.

(1) Coatings and metal

Two types of CP-compatible coatings were selected for the coating disbondment study in this project, as shown in Figure 2. A liquid epoxy coating (3M™ Scotchkote™ 323+), a two-part system designed to protect steel pipe from the harsh effects of corrosion, is used as one representative of a CP-compatible coating. 100 coating panels of this epoxy coating have been prepared in the lab for testing in this reporting period. The average coating thickness of this liquid epoxy coating is around 15 mil.

The second representative of a CP-compatible coating—fusion bonded epoxy (FBE) was purchased from Midwest Coating Company. The coating samples are customized and designed to have a one-layer FBE coating with a thickness of around 15 mil on a Q-panel substrate. 100 coating panels were purchased from the company. The FBE coating samples are divided into two categories: coating with defects and coating without defects based on their initial electrochemical impedance modulus tested by electrochemical impedance spectroscopy.

The Q panel (S36) is chosen as the substrate for the coatings because S36 panels are produced to have excellent chemical resistance, weathering and corrosion resistance, and physical properties. Thus S36 Q panel is commonly used as the metal substrate for corrosion protective coatings.

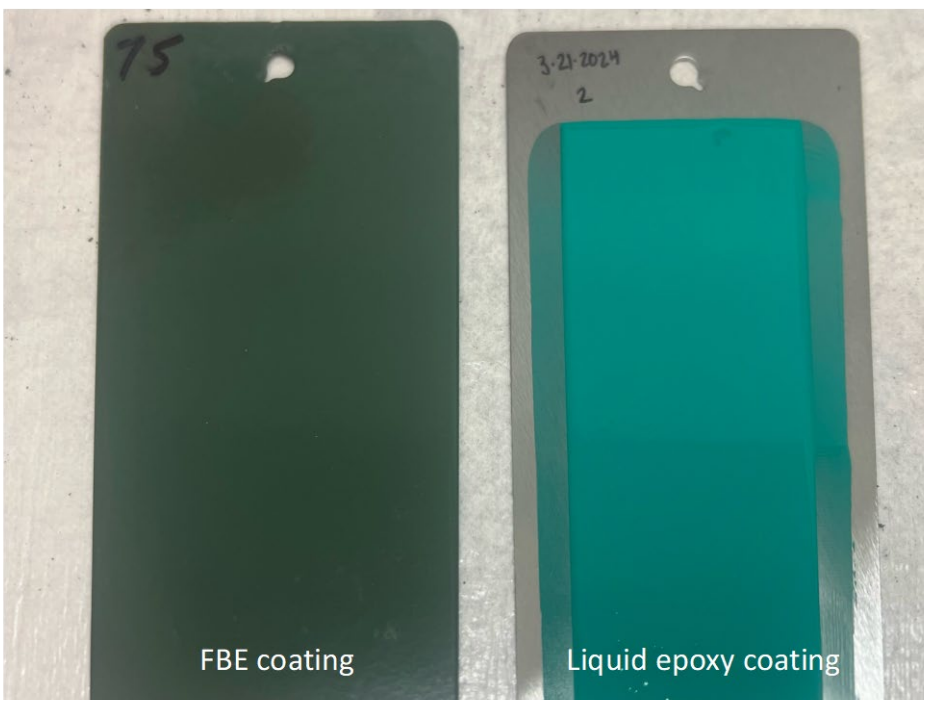

Figure 2. Perfect coating samples of FBE coating and liquid epoxy coating.

(2) Solution

A 3 wt.% NaCl solution is selected as the testing media according to ASTM G8, ASTM G95, and NACE TM0015 standards. The solution is prepared by adding NaCl solids into the deionized water. The pH of the 3 wt.% NaCl solution is around 5.9.

(3) Initial disbondment diameter

The initial disbondment is artificially made by drilling a hole in the coating surface, as specified by the standards. The fully cured coating panel is drilled in the middle of the surface to get a holiday around 3.2 mm (0.125 in) in diameter, based on ASTM G95. The exposed area is then cleaned with isopropyl alcohol and blown with air to dry. The exact diameter and the exposed area are measured by using an OLYMPUS stand scope. An example of these coating samples with the artificial hole is shown in Figure 3.

(4) Cathodic protection conditions

The cathodic potential used for coating the cathodic disbondment study is -0.775, -1.5, and -2.923 V vs. SCE. The three CP potentials are the representatives of the standard value of CP, medium value of CP, and high value of CP to cover the used CP potential range including the reported over-protection level. The coating samples are exposed to the CP conditions under different durations (3, 7, 14, 21 days, and 2 months). This duration time includes short-term and long-term periods to provide a systematic study.

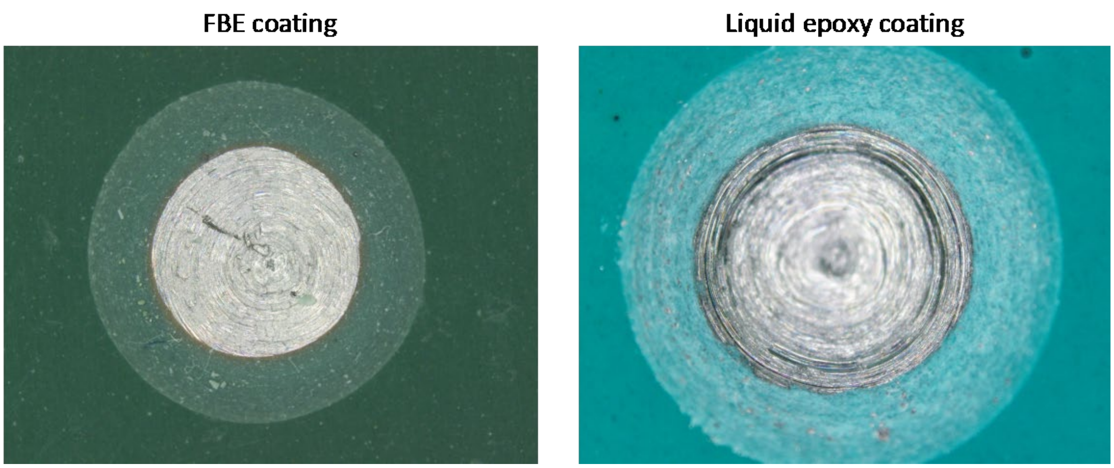

Figure 3. Coating samples with an artificial hole of FBE coating and liquid epoxy coating.

(5) Coating characterization

The experimental setups for applying CP while monitoring coating disbondment behavior have been designed and used for the testing, as shown in Figure 4. The open circuit potential is conducted before and after the cathodic disbondment test. Besides, the electrochemical impedance spectroscopy is performed before and after the test. The local pH around the disbondment area is measured by a micro pH meter. The disbonded area of the coating surface is characterized by optical microscopy and analyzed using ImageJ software. Blisters or rusts are visually inspected and recorded followed by a cathodic disbondment test.

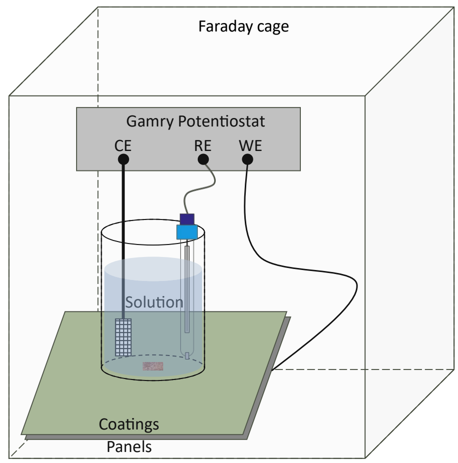

Figure 4. The electrochemical cell for the coating cathodic disbondment test. S type Q-panel as working electrode (WE), saturated calomel electrode as reference electrode (RE), and platinum sheet as counter electrode (CE).

2.2.2. Experimental protocol for the study of coating cathodic disbondment

The experimental testing protocol is designed to study the coating cathodic disbondment, as illustrated in Figure 5. The fully cured coating panel is measured for thickness. Then, an artificial defect is performed according to ASTM G95 to generate a holiday with 0.125 inches in diameter. The coating surface is captured for its initial image. Next, the electrochemical cell is filled with a 3 wt.% NaCl solution. The pH of the solution as well as the initial electrochemical impedance of the coating sample is measured. After the EIS test, open circuit potential (OCP) is conducted and run for 30 minutes. Then, the cathodic protection is applied to the coating sample through Potentiostat. After applying cathodic protection for the designed time, the electrochemical cell (coating sample) is tested for its OCP for 30 minutes to several hours until it reaches a stable potential. Also, the pH of the solution in the electrochemical cell after cathodic protection is monitored. The EIS is also measured. Finally, the coating sample is removed from the test cell. The coating cathodic disbondment area is analyzed using Image J software. Blisters or rust on the coating surface are inspected and recorded, and the image of the coating is captured.

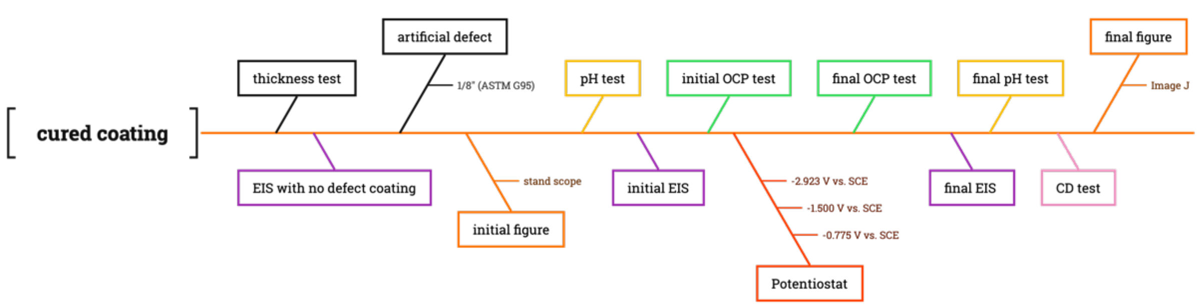

Figure 5. Experimental protocol for the study of coating cathodic disbondment.

The coating cathodic disbondment testing procedure is illustrated in Figure 6. It includes the experimental setup for the electrochemical cell, CP potential conditions, and how to identify the disbonded area after the cathodic disbondment test.

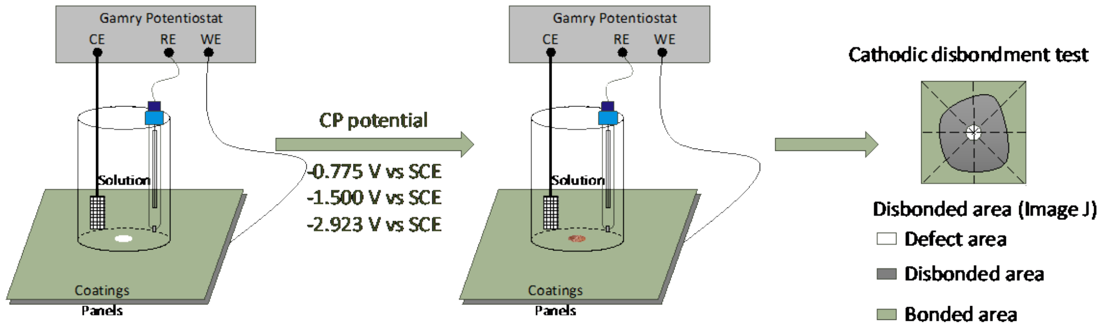

Figure 6. Coating cathodic disbondment testing procedure.

2.2.3. Results

The liquid epoxy coating and the FBE coating are studied for the coating cathodic disbondment under different CP levels according to the experimental setup and testing procedures. An example of the testing for liquid epoxy under different CP levels is shown in Figure 7. After the disbondment testing, the coating surface and the disbonded area are evaluated, as shown in Figure 8. It is clear that the coating disbondment area increased with higher CP levels. The relationship between the coating disbondment area, the duration time, and the CP levels need to be further investigated.

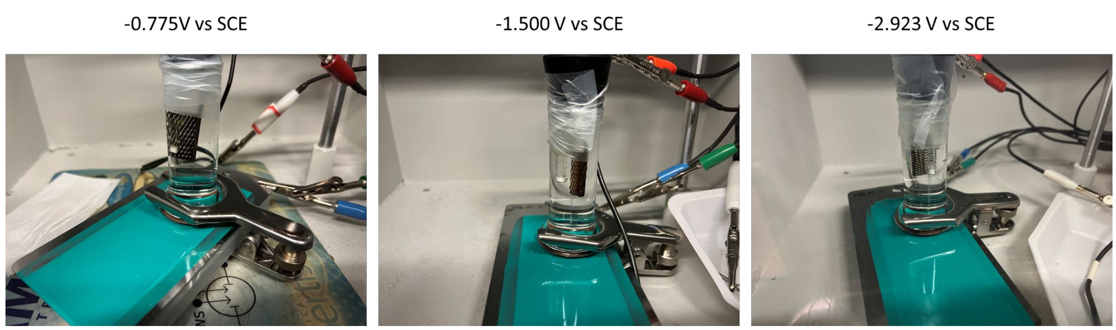

Figure 7. Cathodic disbondment testing of the liquid epoxy coating under different CP potential conditions of -0.775 V, -1.500 V, and -2.923 V vs SCE.

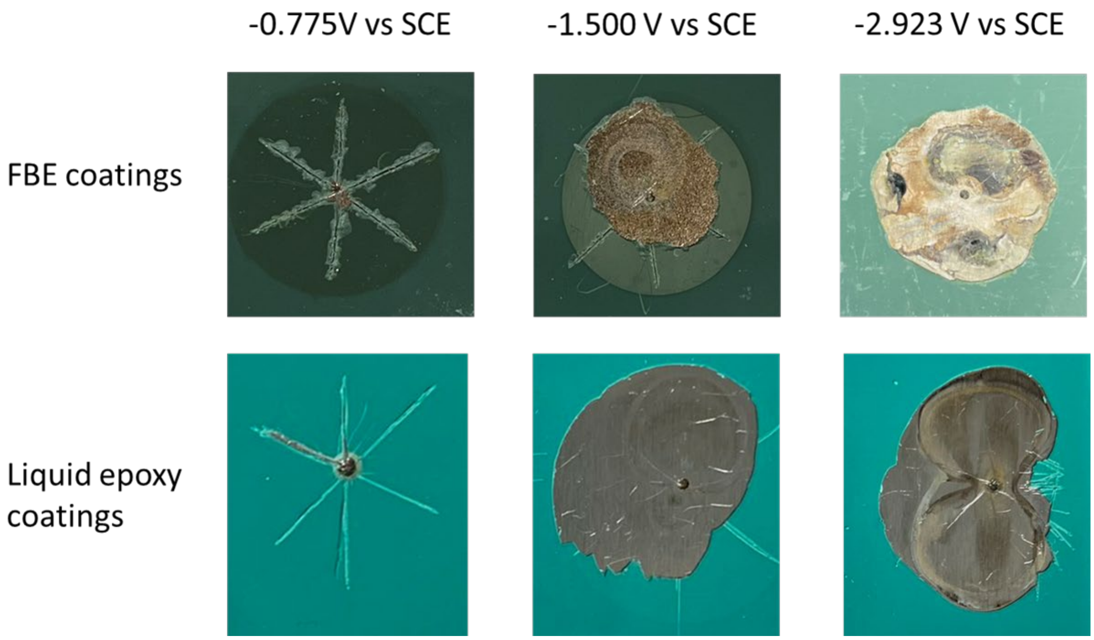

Figure 8. Cathodic disbondment test results of FBE coatings and liquid epoxy coatings under different CP potential conditions of -0.775 V, -1.500 V, and -2.923 V vs SCE.

2.3. Conclusions

The experimental setups and testing procedures for the study of coating cathodic disbondment have been designed and established. Two CP-compatible coatings have been identified, prepared, and started testing. The characterization methods for coating cathodic disbondment have been selected and are ready for the study.

2.4. Future Work

A systematic study for coating cathodic disbondment will be undertaken. It includes different CP levels, different duration time, and different coating types as the key influencing factors. The evaluation includes the cathodic disbondment area, pH of the solution, OCP, impedance by EIS, and surface profile.

3. Task 3. Numerical Simulation of Pipeline Coating Disbondment Behavior and CP System

3.1. Background and Objectives in the 2nd Annual Report Period

CP safeguards steel pipelines by applying an electric current, thereby effectively preventing corrosion. According to the developmental mechanism of cathodic disbondment (CD), CD is often initiated by the formation of holidays caused by accidental coating damage, indicating that coating delamination typically occurs after the formation of holidays. Meanwhile, once disbondment forms, holidays serve as channels and pathways for CP current flow and particle exchange. Therefore, integrating holidays and disbondment into a model is essential for accurately modeling CD scenarios, enabling a more precise investigation of the electrochemical processes within the CD system and evaluation of the effectiveness of CP.

In this task, a numerical model integrating coating holiday and disbondment was established to investigate corrosion on pipeline surfaces under the influence of CP, as well as to analyze particle exchange and distribution within the system. Given that pH is a critical factor influencing the progression of disbondment based on experiment studies in the literature, the analysis will be conducted to investigate the effects of various influence factors on pH distribution.

3.2. Research Progress in the 2nd Annual Report Period

3.2.1. Model setups

(1) Model geometry

The schematic representation of the crevice geometry employed in the model proposed in this study is illustrated in **Figure 9**. The system is symmetric about the line OY, and the analysis focuses on this symmetric cross-section. The domain of the disbonded coating system (OABCDEFG) is partitioned into two regions: the holiday (OABCDG) and the disbondment (DEFG). The boundaries of the system include the symmetry line OB, the metal surface OF, and the coating sections CD, DE, and EF, as well as the holiday opening BC.

To simplify the model calculations, the following assumptions are considered:

1. The disbondment is simplified to a narrow rectangular shape, and the parts of the pipeline with well-adhered coating are excluded from the system. It is assumed that the coating is impermeable to both current and oxygen. During cathodic protection of the metal surface within the disbonded coating system, current flows through the electrolyte within the holiday and disbondment to reach the metal surfaces.

2. Concentration gradients are considered negligible at distances far from the metal surface. This assumption introduces a boundary known as the bulk boundary, where both species concentration and potential are held constant. In this model, the bulk boundary is defined at the opening of the holiday.

3. The crevice is initially filled with a neutral sodium chloride electrolyte with minimal ferrous content, and the bulk solution outside the holiday is assumed to be saturated with oxygen from the

air at 25°C and 101.3 kPa. Homogeneous reactions were not considered in this analysis.

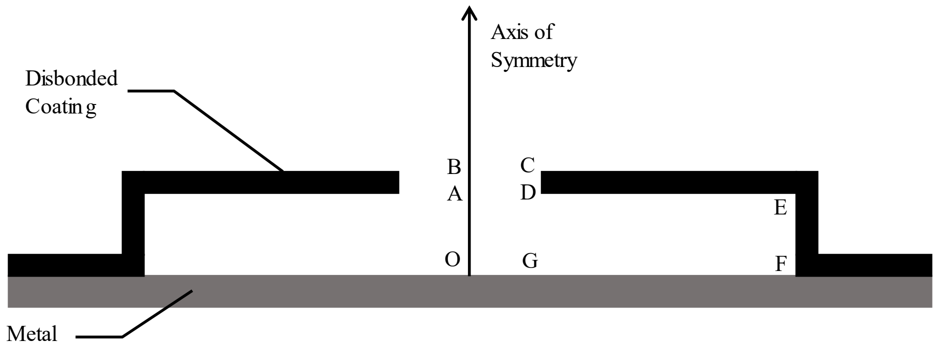

Figure 9. Schematic diagram of the simulation domain.

(2) General transport equations

In dilute electrochemical systems, the steady-state mass conservation equation governs the concentration of each species c_i:

$$0 = -\nabla \cdot N_i + R_i \qquad (1)$$

where N_i is the net flux of species i and R_i is the rate of production or depletion of species i by chemical reactions which can be given by

$$R_i = \frac{i_{net}}{nF} \qquad (2)$$

where i_{net} is the current density of the reaction; n is the number of charges transferred in the reaction; and F is Faraday's constant (96500 C/mol).

The term of flux N_i in **Equation 1** is given by the Nernst-Plank equation, which consists of contributions from migration, diffusion, and convection:

$$N_i = -z_i u_i c_i F \nabla \Phi - D_i \nabla c_i + c_i v \qquad (3)$$

where c_i is the concentration of species i; Φ is the local electrolyte potential; z_i is the ionic charge number of species i; u_i is the mobility; D_i is the diffusion coefficient; and v is the convection velocity of electrolyte.

Under the assumption that the electrolyte is stagnant, the term of convection is negligible, **Equation 3** is recast as:

$$N_i = -z_i u_i c_i F \nabla \Phi - D_i \nabla c_i \qquad (4)$$

The term for mobility u_i can be rewritten using the Nernst-Einstein equation as follows:

$$u_i = \frac{D_i}{RT} \qquad (5)$$

where R is the molar gas constant (8.314 J/(mol·K)) and T is the absolute temperature (298K).

By combining **Equations 1, 2, 4, and 5**, the general steady-state governing equation for species transport is obtained:

$$0 = \frac{z_i F}{RT} D_i \left(\frac{\partial c_i}{\partial x}\frac{\partial \Phi}{\partial x} + c_i \frac{\partial^2 \Phi}{\partial x^2}\right) + D_i \frac{\partial^2 c_i}{\partial x^2} + \frac{i_{net}}{nF} \qquad (6)$$

(3) Electrochemical kinetic equations

Electrochemical reactions occur at the surface of the pipeline, including both anode metal dissolution and cathodic reactions, which encompass oxygen reduction and hydrogen evolution:

Anode: $Fe \rightarrow Fe^{2+} + 2e^-$

Cathode: $O_2 + 2H_2O + 4e^- \rightarrow 4OH^-$

$2H_2O + 2e^- \rightarrow 2OH^- + H_2$

The Tafel equations are applied for different reactions:

$$i_{Fe} = i_{Fe}^0 \times 10^{\frac{\eta_{Fe}}{A_{Fe}}} \qquad (7)$$

$$i_{O_2} = \frac{c_{O_2}}{c_{O_2}^{ref}} \times i_{O_2}^0 \times 10^{\frac{\eta_{O_2}}{A_{O_2}}} \qquad (8)$$

$$i_{H_2} = i_{H_2}^0 \times 10^{\frac{\eta_{H_2}}{A_{H_2}}} \qquad (9)$$

where, i_{Fe}^0,$i_{O_2}^0$and $i_{H_2}^0$ are the exchange current densities for the anodic and cathodic reactions, c_{O2} is the concentration of the diffusing oxygen at the pipe level, $c_{O_2}^{ref}$ is the reference oxygen concentration at bulk electrolyte, A_{Fe}, A_{O2}, and A_{H2} are the anodic and cathodic Tafel slopes. The η_{Fe}, η_{O_2}, and η_{H_2} are the anodic and cathodic over-potentials.

(4) Boundary conditions

According to the assumption, the bulk boundary is positioned at the opening of the holiday. At this boundary, specifically at the mouth of the holiday (BC), the values of c_i and Φ are set to their respective bulk conditions, $c_{i,\infty}$ and Φ_∞, and are maintained as constant. A solution potential of $\Phi_\infty = 0$ was chosen, establishing a reference zero for the Φ values calculated within the model at the bulk boundary.

Natural boundary conditions were employed for c_{Na+}, c_{Cl-}, c_{OH-}, and c_{Fe+2} at all boundaries except at the mouth. At the boundaries associated with the coating (CD, DE, and EF) and the line of symmetry AB, a no-flux condition was imposed, defined by

$$N_i \cdot n = 0 \qquad (10)$$

where n was the unit vector normal to the surface.

3.2.2. Methods of solving the model

The equations described in the model consist of second-order nonlinear partial differential equations and algebraic equations. Due to the coupling between species concentration c_i and potential Φ, analytical solutions are not feasible, necessitating numerical methods for solution. Typically, the Finite Difference Method (FDM) is used for such purposes. This process involves applying dimensionless transformations to the equations and their associated initial and boundary conditions, followed by setting up spatial and temporal grids. Numerical iterative techniques are then employed to solve the equations. In this study, the commercial finite element software COMSOL 6.2 will be used to perform the numerical simulations. The parameters used for this simulation are detailed in Table 4.

Table 4. The parameters used in the model.

Symbol	Values	Expression
r_h (cm)	0.25	Holiday radius
r_d (cm)	1.0	Disbondment length
g (cm)	0.05	Disbondment gap
D_{Na+} (cm^2/s)	1.334×10^5	Diffusion coefficient of Na^+
D_{Cl-} (cm^2/s)	2.034×10^5	Diffusion coefficient of Cl^-
D_{OH-} (cm^2/s)	5.246×10^5	Diffusion coefficient of OH^-
D_{Fe2+} (cm^2/s)	0.712×10^5	Diffusion coefficient of Fe^{2+}
D_{O2} (cm^2/s)	2.781×10^5	Diffusion coefficient of O_2
$c_{Na+,\infty}$(mol/L)	10^{-3}	Concentration of Na^+ in the bulk solution
$c_{Cl-,\infty}$(mol/L)	10^{-3}	Concentration of Cl^- in the bulk solution
$c_{OH-,\infty}$(mol/L)	10^{-7}	Concentration of OH^- in the bulk solution
$c_{Fe2+,\infty}$(mol/L)	10^{-15}	Concentration of Fe^{2+} in the bulk solution
$c_{O2,\infty}$(mol/L)	2.7×10^{-4}	Concentration of dissolved oxygen in the bulk solution
η_{Fe} (V)	-0.76	Standard potential of metal dissolution reaction
i^0_{Fe} (A/m^2)	7.1×10^{-5}	Exchange current density of metal dissolution reaction
A_{Fe} (V/decade)	0.06	Tafel slope of metal dissolution reaction

η_{O2} (V)	0.189	Standard potential of oxygen reduction reaction
$i^0_{O_2}$ (A/m^2)	7.7×10^{-7}	Exchange current density of oxygen reduction reaction
A_{O2} (V/decade)	-0.12	Tafel slope of oxygen reduction reaction
η_{H2} (V)	-1.03	Standard potential of hydrogen evolution reaction
$i^0_{H_2}$ (A/m^2)	1.1×10^{-2}	Exchange current density of hydrogen evolution reaction
A_{H2}	-0.15	Tafel slope of hydrogen evolution reaction

3.3. Conclusions and Future work

With the developed model, the main outputs include CP potential distribution, local current density for assessing local corrosion, and pH distribution for assessment of coating disbandment potential. In the model design, the following parameters will be altered to study the effects of these variations on the outputs.

The magnitude of the CP potential can affect the effectiveness of CP protection, especially in cases such as crevice corrosion. The shape of crevice due to coating disbandment is also commonly used as a controlled variable in these studies. The gap and depth of coating holiday mainly affect the distribution of CP and the transportation of particles in the electrolyte. Additionally, the consideration of the presence and concentration of oxygen, which is one of the reactants in the cathodic reaction, is also an important factor. Furthermore, factors such as soil electrical conductivity will be considered. Various soil electrolytes within the crevice can influence the distribution of CP. Different steel materials exhibit diverse polarization characteristics, potentially impacting the effectiveness of CP from a material standpoint.

4. Task 4. Probabilistic Degradation Model of Coated Pipe Wall Due to Excessive CP

4.1. Background and Objectives in the 2nd Annual Report Period

Cathodic disbondment (CD) has been recognized as the main cause of coating degradation for coated pipelines exposed to cathodic protection (CP) [10]. The objective of Task 4 in this reporting period is to understand the mechanism of coating disbondment under CP and identify the possible influence of different factors to prepare for the next step of modeling of time-evolution of cathodic disbondment.

4.2. Research Progress in the 2nd Annual Report Period

4.2.1. CD Rate

It is generally accepted that CP in pipelines may result in the formation of subproducts that can affect the adhesion of the coating around the defect and cause CD in the coated pipelines. This delamination can be further promoted under cathodic overprotection [11].

Previous work has used different CD standardized tests to evaluate coating resistance to CD [11-14]. In order to measure this resistance, the disbondment radius has been used as the reference parameter of CD [10]. Figure 10 shows an example of the area affected by CD in a coating exposed to CP during a CD test. In general, after the CD test is performed, the coating disbondment is determined by making radial direction cuts through the drilled holiday, and then the coating at the holiday is lifted to expose the disbonded area. The CD length is calculated as follows [15]:

Disbondment radius = (average of disbondment diameters −holiday diameter) / 2

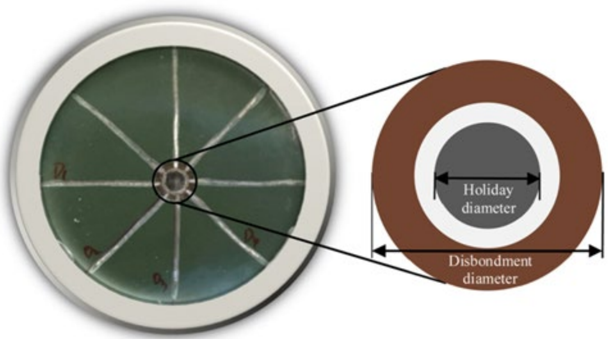

Figure 10. Representation of the area affected by CD in a coating exposed to CP.

The duration of the CD test should be considered, as it can differentiate the disbondment results among different studies [10]. To compare CD results, the cathodic disbondment rate (i.e., CD rate) is obtained by normalizing the disbondment results (disbondment radius) with respect to the time of testing. In this stage, the CD rates from various tests are collected from the literature review ([11-14, 16]). Under different CP potential, electrolyte pH, and coating thickness conditions, one can examine how these factors influence the CD rate, as shown below.

4.2.2. CP potential

It is widely accepted that CP potential influence on CD behavior. According to the previous study ([10, 11, 13]), disbondment areas increase as the applied CP potentials increase. Thus, it is expected that the CD rate also increases as the CP potential increases.

Figure 11 shows the variation in the CD rate as the changes in CP potential, considering different coating types. Not much data is available for CP levels larger than -1.5 V vs. SCE, as -1.5 V vs. SCE is the CP reference value suggested by the different CD standard tests. In general, for all coatings, the CD rate increases as CP potential becomes more negative. However, no insights related to the CP potential influence can be derived from the Solid Epoxy coating specimens as the CP potential for this coating was constant. For the studies that considered CP values more negative than -1.5 V vs. SCE, significantly higher CD rate results are observed. On the other hand, it is known that coating type has an impact on the disbondment response to the same CP potential; thus, more data that considers a wider range of CP potential levels for the same coating is needed to quantify the influence of CP levels on the CD rate.

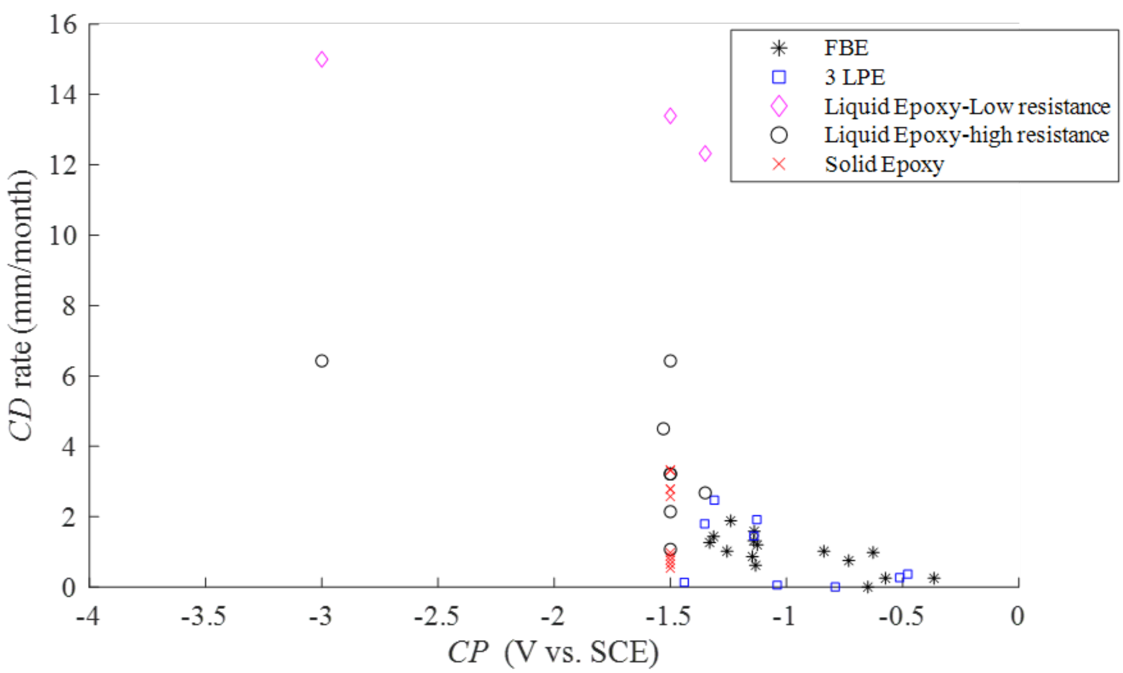

Figure 11. CD rate vs. CP level for different coating types.

4.2.3. Electrolyte pH

The pH level in the electrolyte around a coating holiday has been previously monitored during CD testing ([11, 12, 16]). It is believed that the cathodic reaction produces subproducts with high pH (alkaline), these subproducts located under the coating can lead to disbonding [10]. Then, it is expected that high pH levels are related to high levels of CD.

Figure 12(a) shows the variation in CD rate as the CP level changes for different levels of electrolyte pH. Figure 12(b) shows the data from Figure 12 but excludes the points where the pH level is unknown. In general, Figure 12(b) shows higher CD rate levels as the electrolyte pH level increases, except for the data corresponding to pH > 9. For data with pH > 9, two regions with different CD rate values are observed, which are circled in Figure 12(b). The data in Region 1 has a much higher CD rate than Region 2. It turns out that the data in these 2 regions corresponds to two different coating types with different chemistry compositions. It is found that the coating for the data in Region 1 refers to a coating with high resistance to disbondment, which could explain the low CD rate for Region 1. These results suggest that more data that considers different electrolyte pH levels for the same coating type is needed to quantify the influence of the electrolyte pH on the CD rate.

4.2.4. Coating thickness

It is believed that the CD rate decreases with thicker film coating, based on the assumption that the coating CP permeability depends upon coating thickness [4]. Some previous studies (e.g., [12-14]) have performed CD testing on coatings with different thicknesses.

Figure 13(a) shows the variation in CD rate vs CP for different coating thicknesses. Figure 13(b) shows the data from Figure 13 but excludes the points where the coating thickness is unknown. Higher CD rate levels are observed for coating thickness between 100-300 μm compared to thickness between 300-500 μm. Contrary to the expected, higher CD rate levels are observed for the thickness between 500-900 μm. It is also found that the data with a thickness between 500-900 μm correspond to a coating with low resistance against cathodic disbondment, which could help understand the high CD rates for this group of data. The results suggest that different thicknesses for the same coating are needed to quantify the influence of coating thickness on CD rate.

4.3. Conclusions

Through the current study conducted on Task 4, the phenomenon of CD in pipelines exposed to CP is better understood. From the experimental data collected from the literature review, CP potential, electrolyte pH, and coating thickness were identified as the main parameters that were evaluated under different scenarios. CD rate variation has been evaluated for the different scenarios of CP potential, pH, and coating thickness, but the data is still scarce in accurately quantifying the influence of these parameters on CD behavior.

4.4. Future Work

Based on these preliminary results, there is a need to collect more data that considers broad ranges of CP potential, electrolyte pH, and coating thickness for the same coating type in order to confirm the influence of these conditions on CD rate. This will be done with further data collection from the literature review and the data that are generated in Tasks 2 and 3. In particular, the experimental research that is conducted in Task 2 considers different CP levels (-0.775, -1.5, and -2.923 V vs. SCE) and two coating types: liquid epoxy and fusion bonded epoxy (FBE) coatings. With a comprehensive database, a prediction model of CD rate will be developed with consideration of all possible influencing factors.

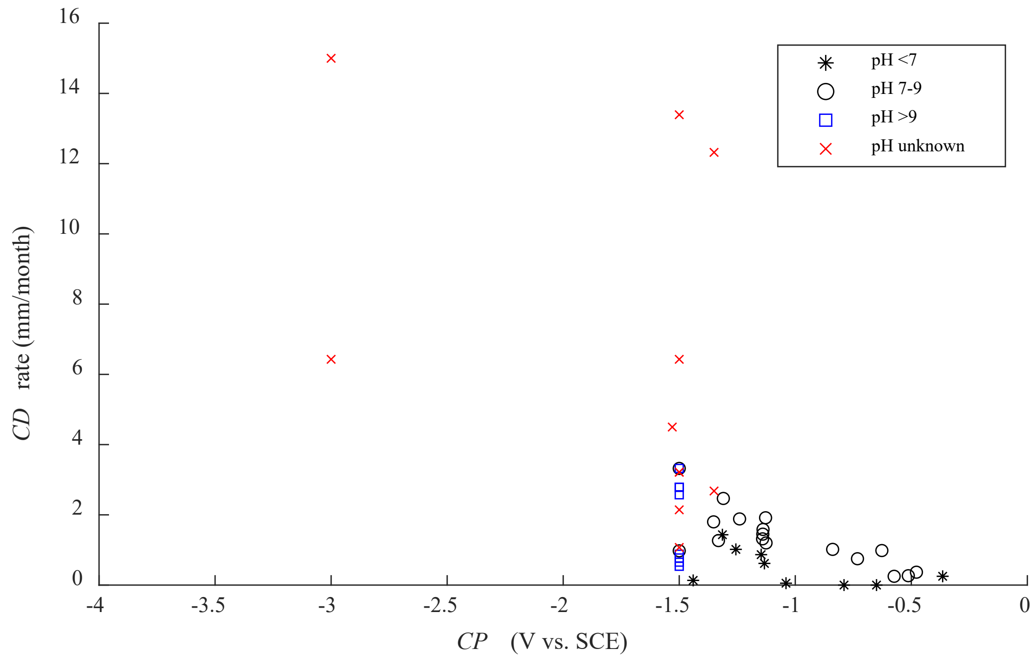

(a) <u>all data</u>

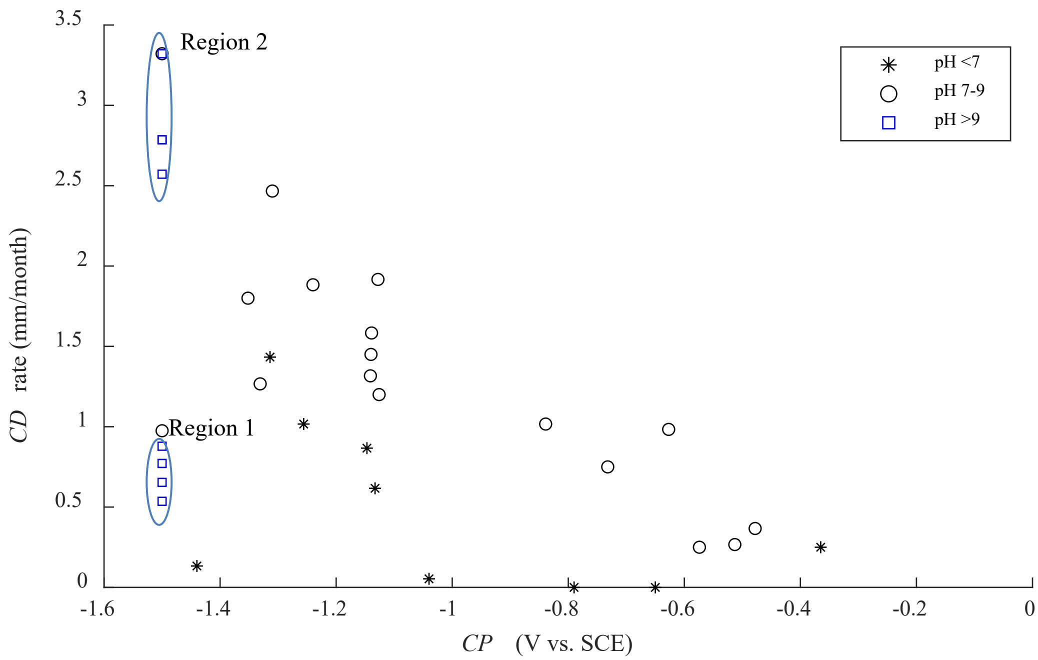

(b) <u>data with known pH and CP < -1.5V</u>

Figure 12. CD rate vs CP level for different levels of pH.

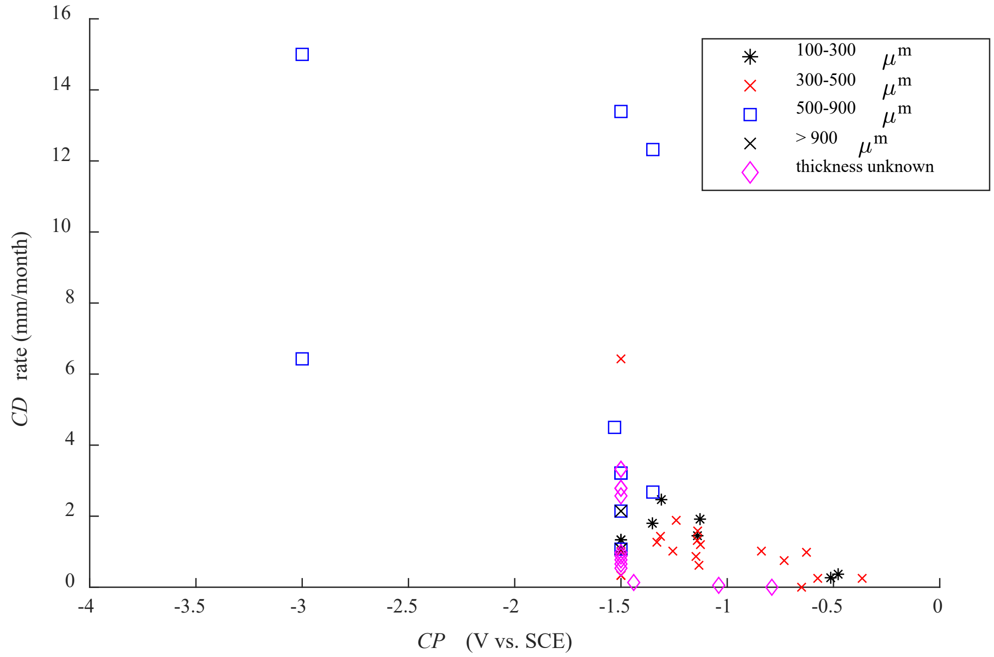

(a) all data

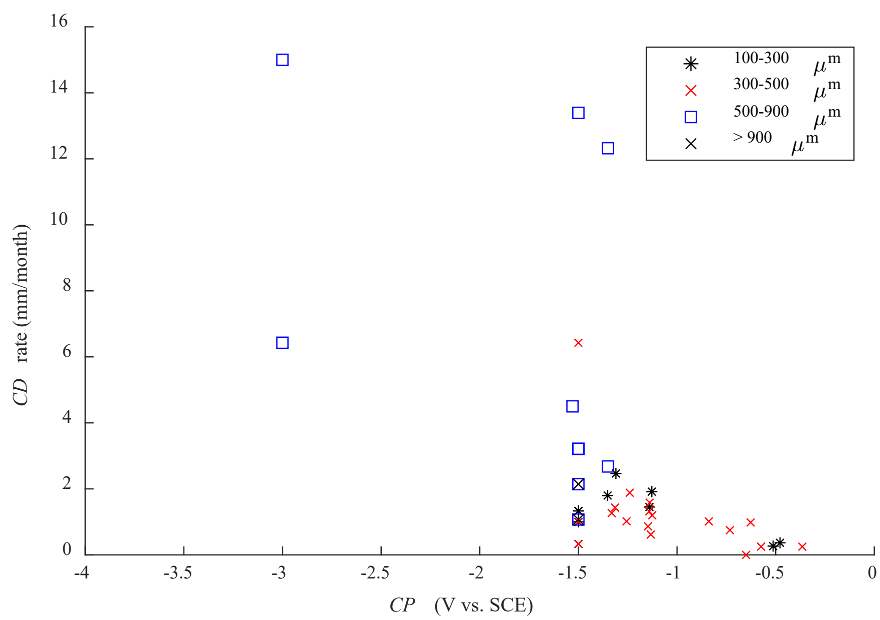

(b) data with known coating thickness

Figure 13. CD rate vs CP level for different values of coating thickness.

5. Task 5. Determination of Recoating Time Using Reliability-based Approach

Task 5 will start in the 9th quarter of this project.

6. Task 6. Industrial Collaborations

The PIs contacted external partners from the oil and gas pipeline industry for industrial collaborations during this reporting period. We sent a survey to pipeline companies to acquire field information. The details of the survey are included in the Appendix. We also talked to experts in pipelines at the annual 2024 AMPP conference and 2024 IPCE conference.

We received vintage pipes with coating from Dr. Rafael Rodriguez through his company. Dr. Rodriguez kindly provided us with the CP operation potentials and coating information for these pipe samples.

References

[1] D. Kuang, Y.F. Cheng, Study of cathodic protection shielding under coating disbondment on pipelines, Corrosion Science, 99 (2015) 249-257.

[2] C. Gu, J. Hu, X. Zhong, The coating delamination mitigation of epoxy coatings by inhibiting the hydrogen evolution reaction, Progress in Organic Coatings, 147 (2020) 105774.

[3] D. Kuang, Y.F. Cheng, Effect of alternating current interference on coating disbondment and cathodic protection shielding on pipelines, Corrosion Engineering, Science and Technology, 50 (2015) 211-217.

[4] K. Yin, Y. Yang, Y. Frank Cheng, Permeability of coal tar enamel coating to cathodic protection current on pipelines, Construction and Building Materials, 192 (2018) 20-27.

[5] J.E. Edy, H.N. McMurray, K.R. Lammers, A.C.A. deVooys, Kinetics of corrosion-driven cathodic disbondment on organic coated trivalent chromium metal-oxide-carbide coatings on steel, Corrosion Science, 157 (2019) 51-61.

[6] J. Wang, J. Hu, C. Gu, Y. Mou, J. Yu, X. Zhong, The effect of pulse current cathodic protection on cathodic disbondment of epoxy coatings, Progress in Organic Coatings, 170 (2022) 107001.

[7] Y. Zhang, One Hundred Percent Solids Ambient Cure Liquid Pipe Coating With Excellent Cathodic Disbondment Results, in: NACE CORROSION, 2019, pp. Paper No. 12823.

[8] F. Akvan, J. Neshati, J. Mofidi, An electrochemical measurement for evaluating the cathodic disbondment of buried pipeline coatings under cathodic protection, Iran. J. Chem. Chem. Eng., 34 (2015) 83-91.

[9] G.R. Ruschau, Y. Chen, Determining the CP Shielding Behavior of Pipeline Coatings in the Laboratory, in: NACE CORROSION 2006, pp. Paper No. 06043.

[10] M. Xu, C.N.C. Lam, D. Wong, E. Asselin, Evaluation of the cathodic disbondment resistance of pipeline coatings – A review, Progress in Organic Coatings, 146 (2020) 105728.

[11] D.S. de Freitas, S.L.D.C. Brasil, G. Leoni, G.X.d. Motta, E.G.B. Leite, J.F.P. Coelho, Long-term cathodic disbondment tests in three-layer polyethylene coatings, Materials and Corrosion, 74 (2023) 1159-1168.

[12] E. Diler, K. Pelissier, A. Meroufel, N. Larche, Investigation of the Mechanisms and Kinetic of Cathodic Disbondment in Seawater and Soils, in: AMPP CORROSION, 2023.

[13] L. Erickson, E. Lemieux, Factors Affecting the Performance of Epoxy Coatings in Cathodic Disbondment, in: SSPC 2018 Conference, New Orleans, 2018.

[14] J. Holub, D.T. Wong, M. Tan, Analysis of CDT methods and factors affecting cathdoic disbondment, in: NACE CORROSION, 2007, pp. Paper No. 07022.

[15] K. Cameron, D. Wong, J. Holub, Practical Analysis of Cathodic Disbondment Test Methods, in: NACE CORROSION, 2005, pp. Paper No. 05029.

[16] A. Al-Borno, M. Brown, S. Rao, The Effect of Anode Isolation Methods on Coating Cathodic Disbondment, in: NACE CORROSION, 2008, pp. Paper No. 08007.

Q1 - 1. Please provide your company name

1. Please provide your company name

SoCalGas

Flint Hills Resources

Boardwalk Pipeline

Marathon Pipe Line LLC

ATCO

Q2 - 2. Please list out the coating type(s) that have been used in the vintage pipelines (that could be over 30 years old)?

2. Please list out the coating type(s) that have been used in the vintage pipelines (that could be over 30 years old)?

Somastic,Wrapped,Coal Tar, Bitumastic, Fusion Bonded Epoxy,Asphalt, Paint, Coal Tar Enamel #7, XTru-Coat, Unknown, Epoxy, Concrete, Coal Tar Enamel #9, Multi-Part Liquid Epoxies, Enamel, Coal Tar Enamel, Mastic, Polypropylene, Pritec, Tape, Grease Wrap #7, PE Jacket, Wax Tape, Durotex, Polyethylene Tape, Dual Layer FBE, Grease Wraps, Plexcoat, Multi-Layer Wrap, Mastic Tape Wrap, PlexGuard, Powercrete, Other like 1 [2:30 PM] Lor, Eric 2003 and newer: Fusion Bonded Epoxy Absent Wrapped Epoxy Mastic Tape Wrap Bare Unknown Somastic Mastic

Coal Tar Enamel, Polyethylene Tape, Fusion Bonded Epoxy, Extruded Polyethylene,

Coal tar epoxy, coal tar enamel, FBE

Coal tar, asphalt, hot applied wax, cold applied wax, extruded polyethelene, shrink sleeves, FBE

Black tape, YJ, coal tar, wax, asphalt enamel, shrink sleeves

Q3 - 3. Please list out the coating type(s) that have been used within recent 20 years?

3. Please list out the coating type(s) that have been used within recent 20 years?

Fusion Bonded Epoxy, Wrapped, Epoxy, Mastic Tape Wrap, Unknown, Somastic, Mastic

Fusion Bonded Epoxy, two-part liquid epoxy

FBE (for plant and field application), liquid epoxy (mainly for field application)

FBE, liquid epoxy, cold applied wax (tape)

YJ, FBE, denso, YJ2k, shrink sleeves

Q4 - 4. Has your pipeline experienced coating cathodic disbondment issues?

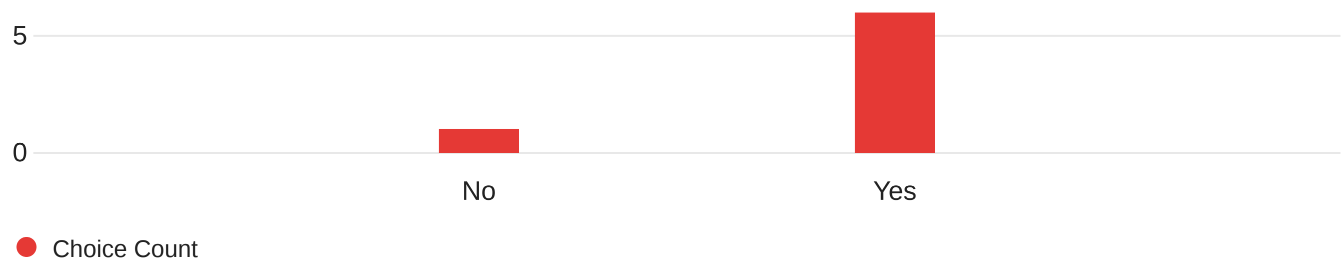

Q14 - Please provide addition information regarding the cathodic disbandment incident. 5. What type of coating is it where the cathodic disbandment incident occurs?

Please provide addition information regarding the cathodic disbandment incident.

5. What type of coating is it where the cathodic disbandment incident occurs?

Haven't categorized. Only categorized by shielding or non-shielding.

Fusion Bonded Epoxy

Coating disbondment has been identified on coal tar and FBE coated pipe. In some cases disbondment could be attributed to CP.

Black tape, shrink sleeves

Q7 - 6. What is the type product transported by the pipeline - Selected Choice

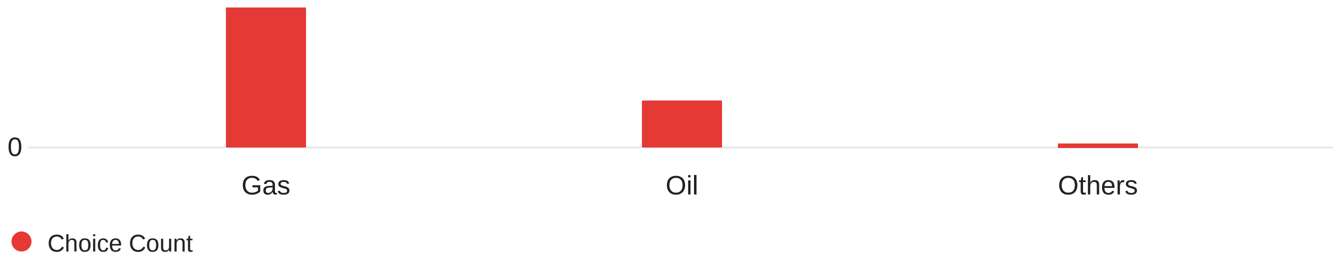

Q8 - 7. Year of pipeline installation

7. Year of pipeline installation
Many vintages
2012
20+
Pre 1970s

Q9 - 8. Was the pipeline subjected to any interference from foreign objects?

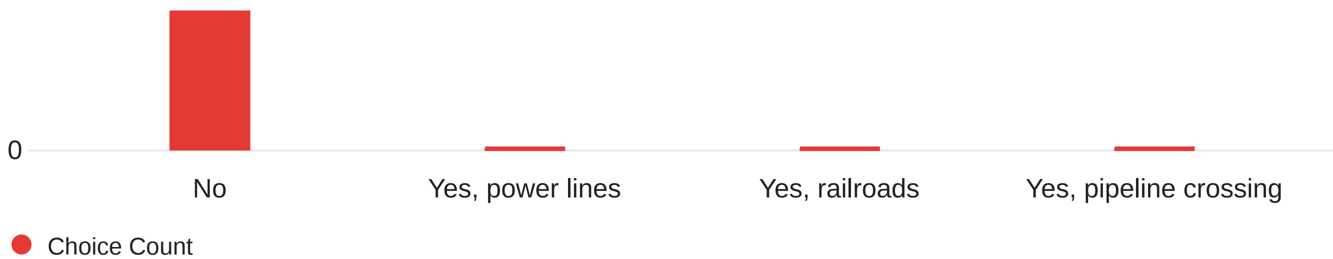

Q11 - 9. Was this pipeline cathodic protected

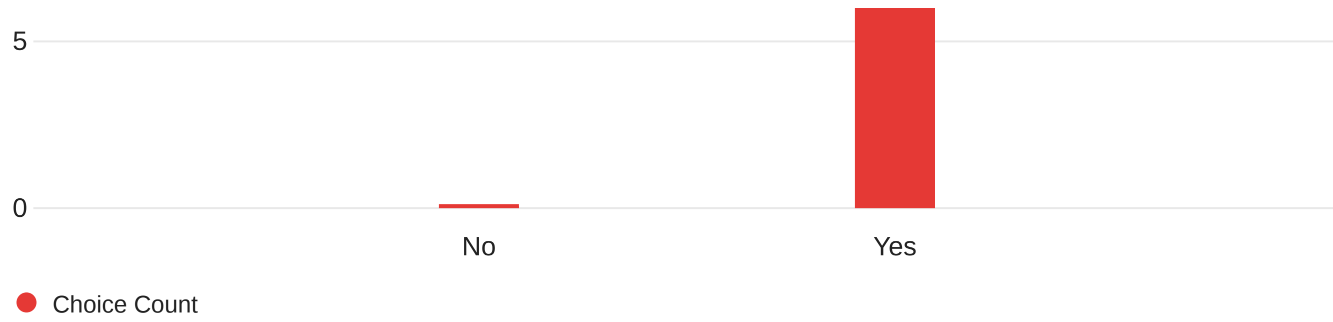

Q12 - 10. What type of cathodic protection is used? And what is the design voltage or current? - Selected Choice

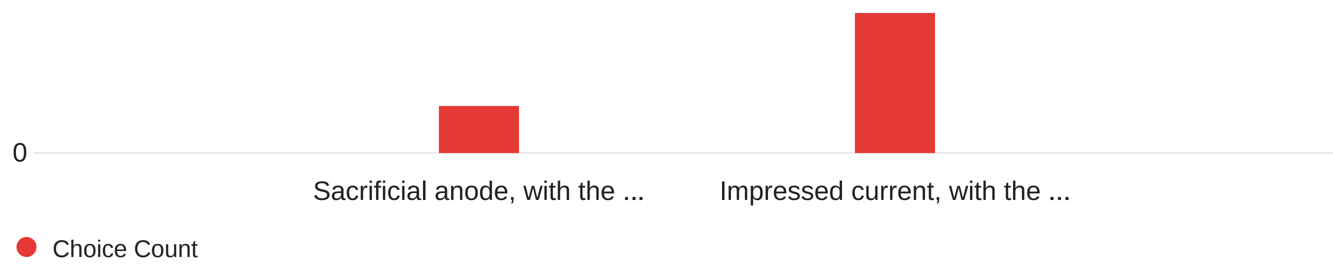

Q13 - 11. Any other information that you would like to add for this cathodic disbondment incident?

11. Any other information that you would like to add for this cathodic disbondment incident?
Coating was about 6 years old when incident was observed. Potentials have run a bit high since new line was built.
Note that coating disbondment can be due to a number of interacting factors. CP is only one of the factors. Metal surface preparation and coating application are other factors that need to be taken into account before assuming that CP was the sole cause of coating disbondment.
Mostly observed with black tape and shrinksleeves. Noted on YJ as well but no noted corrosion as far as i know